

This is the peer reviewed version of the following article:

Reinforcement of EPDM rubber with in situ generated silica particles in the presence of a coupling agent via a sol-gel route / T. H., Mokhothu; A. S., Luyt; Messori, Massimo. - In: POLYMER TESTING. - ISSN 0142-9418. - STAMPA. - 33:(2014), pp. 97-106. [10.1016/j.polymertesting.2013.11.009]

Terms of use:

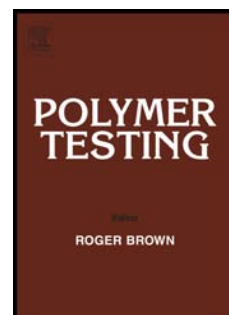
The terms and conditions for the reuse of this version of the manuscript are specified in the publishing policy. For all terms of use and more information see the publisher's website.

18/12/2025 17:13

Accepted Manuscript

Reinforcement of EPDM rubber with *in situ* generated silica particles in the presence of a coupling agent *via* a sol-gel route

T.H. Mokhothu, A.S. Luyt, M. Messori



PII: S0142-9418(13)00237-7

DOI: [10.1016/j.polymertesting.2013.11.009](https://doi.org/10.1016/j.polymertesting.2013.11.009)

Reference: POTE 4158

To appear in: *Polymer Testing*

Received Date: 10 October 2013

Accepted Date: 18 November 2013

Please cite this article as: T.H. Mokhothu, A.S. Luyt, M. Messori, Reinforcement of EPDM rubber with *in situ* generated silica particles in the presence of a coupling agent *via* a sol-gel route, *Polymer Testing* (2013), doi: 10.1016/j.polymertesting.2013.11.009.

This is a PDF file of an unedited manuscript that has been accepted for publication. As a service to our customers we are providing this early version of the manuscript. The manuscript will undergo copyediting, typesetting, and review of the resulting proof before it is published in its final form. Please note that during the production process errors may be discovered which could affect the content, and all legal disclaimers that apply to the journal pertain.

Material Properties

Reinforcement of EPDM rubber with *in situ* generated silica particles in the presence of a coupling agent via a sol-gel route

T. H. Mokhothu¹, A.S. Luyt^{1*}

¹Department of Chemistry, University of the Free State (QwaQwa Campus), Private Bag X13, Phuthaditjhaba, 9866, South Africa

M. Messori²

² Department of Engineering 'Enzo Ferrari', University of Modena and Reggio Emilia, Via Vignolese 905/A - 41125 Modena, Italy

Abstract

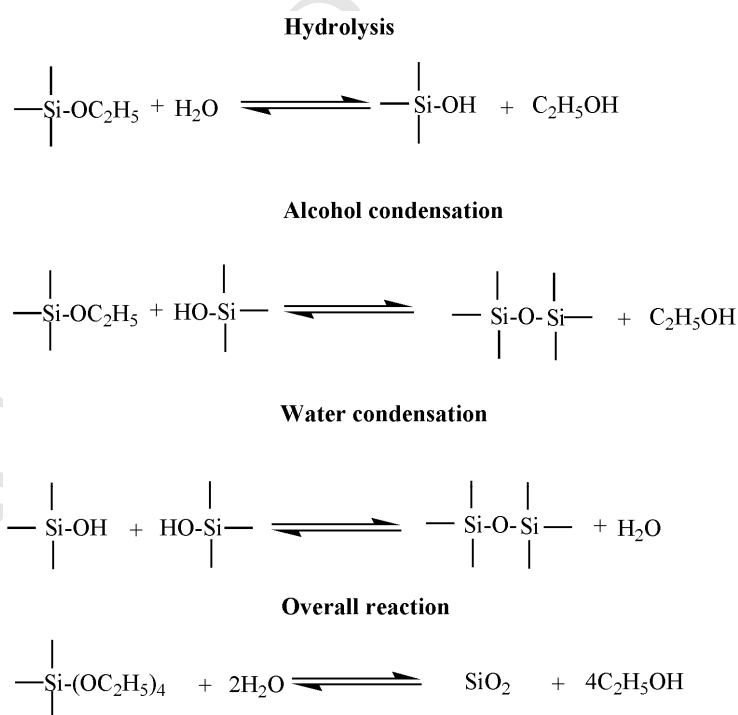
Ethylene propylene diene monomer rubber (EPDM)-silica (SiO₂) composites were prepared by means of an *in situ* sol-gel process with tetraethoxysilane (TEOS) as precursor and bis-[-3-(triethoxysilyl)-propyl]-tetrasulfide (TESPT) as coupling agent. Homogenous dispersion of the silica particles was observed in all cases, as well as good adhesion between the filler and the matrix. The swelling and gel content results indicated that the number of crosslinks decreased, while the network was still extensive enough to maintain the high gel content. These results indicate that the coupling agent acted as a bridge between the hydrophilic silica and the hydrophobic rubber and enhanced the rubber-silica interactions. This enhanced interaction gave rise to increased thermal stability of the EPDM. The values of the Nielsen model parameters, which gave rise to good agreement with the experimentally determined Young's modulus values, indicate improved dispersion and reduced size of silica aggregates in the EPDM matrix. Good agreement was found between the storage modulus and Young's modulus values. The filler effectiveness (Factor C) indicated a mechanical stiffening effect and a thermal stability contribution by the filler, while the damping reduction (DR^{Norm}) values confirmed that the EPDM interacted strongly with the well dispersed silica particles, and the polymer chain mobility was restricted.

Keywords: EPDM; silica; nanocomposites; coupling agent; reinforcement

* Corresponding author (LuytAS@qwa.ufs.ac.za)

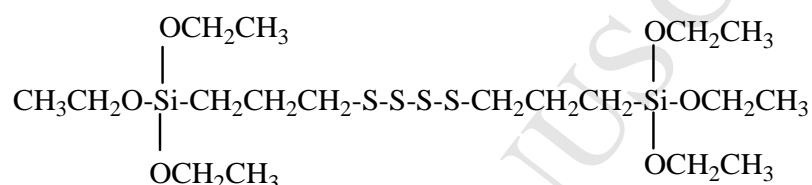
1. Introduction

Growing of *in situ* sol-gel derived inorganic metal oxides (silica, titania, zirconia) is one of the promising routes for producing rubber matrices filled with uniformly dispersed particles [1-8]. However, an important disadvantage of reinforcement with inorganic fillers is their incompatibility with the rubber matrix, which ultimately gives rise to the formation of large aggregates in the matrix. An example is the very strong interaction between silica particles caused by hydrogen bonding of the silanol groups to the silica surface [1,2]. This interaction prevents the filler from uniformly dispersing in the matrix and, therefore, results in the formation of silica aggregates. This problem can be solved by the introduction of different types of silane coupling agents in the sol-gel process during the *in situ* generation, which should make it possible to modify the filler-matrix and filler-filler interactions [1,6,9,10]. The sol-gel reaction of tetraethoxysilane (TEOS) occurs in two steps, hydrolysis and condensation, and results in the formation of SiO₂, as shown in Scheme 1. This application of the sol-gel process in rubber chemistry is related to the use of silane coupling agents and of moisture or silane curing, and it has already been carried out on natural rubber (NR), styrene-butadiene, ethylene propylene diene monomer rubber (EPDM) and butadiene rubber [2-5,9,11-14].



Scheme 1 Sol-gel reaction of trioxysilane (TEOS)

The *in situ* generation of silica reinforced rubber composites using the sol-gel reaction of TEOS in the presence of bis-[3-(triethoxysilyl)-propyl]-tetrasulfide (TESPT) as coupling agent has been reported in several papers [1,6,9,11]. The function of TESPT as a coupling agent is to enhance the rubber-silica interaction by acting as a bridge between the hydrophilic silica and the hydrophobic rubber. The interaction is promoted by two chemically active chemical groups in TESPT, the ethoxy ($\text{CH}_3\text{CH}_2\text{O}-$) and sulphide ($-\text{S}-$) groups, as shown in the structure below. The ethoxy group is capable of reacting with the silanol on the silica surface, whereas the sulphide can participate in sulphur vulcanization leading to a strong chemical linkage between the silane coupling agent and the rubber molecules [11].



Murakami *et al.* [3] investigated the effect of a silane-coupling agent on natural rubber (NR) filled with *in situ* generated silica. They reported that the simultaneous use of *in situ* silica and the silane coupling agent γ -mercaptopropyltrimethoxysilane (γ -MPS) significantly prevented the delay of sulphur curing, and increased the wettability of NR onto *in situ* silica, which resulted in an increase in the reinforcement of the NR vulcanizate. The reinforcing efficiency offered by the *in situ* sol-gel reaction of TEOS in the presence of coupling agents is much higher than that obtained either by conventional mechanical mixing or by the *in situ* reaction without any coupling agent. Studies on the reinforcement of NR, where *in situ* generated silicas and nanofibres of sepiolite were used, indicated that the silica particles generated before vulcanization seem to inhibit the crosslinking reaction of NR by sulphur and form a silica-silica network *via* the silanol groups present on the silica surface. The use of TESPT as silane coupling agent led, however, to a substantial extent of reinforcement [12]. Furthermore, the mixing with the silane coupling agent gave rise to an important decrease in the swelling ratio, which indicated better crosslinking effect between the organic and inorganic components.

Reinforcement of rubber matrices with *in situ* generated inorganic metal oxide by using a sol-gel route is associated with the improvement of properties such as thermal, thermomechanical and mechanical, as well as the morphology and crosslinking efficiency. Studies on EPDM rubber reinforced with *in situ* generated silica [13,14] showed an increased

agglomeration with increasing filler content, as well as a decrease in the crosslinking density of the matrix as a result of the presence of silica particles. In this work, we focused on the preparation of *in situ* silica-EPDM rubber composites by introducing a silane coupling agent bis-[-3-(triethoxysilyl)-propyl]-tetrasulfide in the sol-gel process. The coupling agent was first pre-mixed with the EPDM matrix, followed by the addition of the precursor TEOS, after which the sol-gel reaction was initiated. This approach is expected to reduce the filler-filler interaction and give rise to improved thermal, mechanical and thermomechanical properties, as well as a better morphology and improved crosslinking.

2. Experimental

2.1 Materials

Tetraethoxysilane (TEOS), tin(II)2-ethylhexanoate, dicumyl peroxide, toluene, bis-[-3-(triethoxysilyl)-propyl]-tetrasulfide (TESPT, commonly known as Si-69) and ethanol were all supplied by Sigma-Aldrich. The materials were used as received without further purification. Ethylene propylene diene monomer rubber (EPDM), Polimeri Europa Dutral[®] TER 4038, density 0.91 g cm⁻³, was provided by ATG Italy (Castel d'Argile, BO, Italy).

2.2 Preparation of EPDM/SiO₂ nanocomposites

EPDM rubber was dissolved in toluene (3g/100ml) at room temperature, followed by addition of TESPT (4 wt% with respect to EPDM) under stirring. The EPDM/SiO₂ composites were prepared by the addition of TEOS, H₂O, ethanol and tin(II)2-ethylhexanoate (1:4:4:0.04 mol ratio), respectively, in the EPDM-TESPT solution. The reaction mixtures were magnetically stirred and heated at 80 °C for 20 hours to activate the hydrolytic condensation of TEOS to silica (SiO₂). The solutions were cooled to room temperature, followed by the addition of dicumyl peroxide (DCP) (1 wt% with respect to EPDM) under stirring. The reactions were taken to a rotating evaporator for elimination of about 80% of solvent and other by-products. The samples were obtained by casting the solution in Petri dishes and dried overnight. The cast samples of EPDM/SiO₂ (90/10, 80/20, 70/30 w/w) were vulcanized by compression at 160 °C for 20 min.

2.3 Characterization methods

The morphologies of the EPDM/SiO₂ nanocomposites were examined by a TESCAN VEGA3 scanning electron microscope (SEM) at a voltage of 25 kV. Cross-sections of the samples were coated with gold by an electro deposition method to impart electrical conductivity before the SEM micrographs were recorded.

ATR-FTIR spectra of the pure EPDM and its silica filled composites were obtained using a Perkin Elmer Spectrum 100 FTIR spectrometer. The samples were analyzed over a range of 600-4000 cm⁻¹ with a resolution of 4 cm⁻¹. All the spectra were averaged over 16 scans.

The degree of crosslinking was determined through equilibrium swelling tests by immersing at least three rectangular specimens for each composition in 15 ml of toluene at room temperature for several hours, and the mean values are reported. The solvent was replaced hourly after each measurement to eliminate all uncrosslinked fractions, such as unvulcanized EPDM chains, which could lead to incorrect values of the swelling ratio. Equilibrium swelling was determined until the swollen mass (m_s) reached a constant value, after which the samples were dried to constant mass (dried mass (m_d)) and the absolute swelling ratio (q) was evaluated using Equation 1.

$$q = \frac{m_s}{m_d} \quad (1)$$

The absolute extractable fraction (f), where m_0 is the mass of the sample before immersion in toluene, was determined using Equation 2.

$$f = \frac{m_s - m_d}{m_0} \times 100 \quad (2)$$

The values of q and f were also normalized to the actual EPDM weight. Their values were determined using Equations 3 and 4.

$$q_{EPDM} = \frac{q}{C_{EPDM}} \quad (3)$$

$$f_{EPDM} = \frac{f}{C_{EPDM}} \quad (4)$$

where C_{EPDM} is the weight fraction of EPDM present in the composites. The gel content was determined using Equations 5 to 7, where m_{EPDM} is the mass of EPDM without silica and $\%wt_{EPDM}$ is the weight % EPDM in the composite.

$$m_{EPDM} = m_o \times \%wt_{EPDM} \quad (5)$$

$$\% Extraction = \frac{m_o - m_d}{m_{EPDM}} \times 100 \quad (6)$$

$$\% Gel = 100 - \% Extraction \quad (7)$$

Thermogravimetric analysis (TGA) was performed with a Perkin Elmer STA6000 simultaneous thermal analyzer. The analysis was done under nitrogen at a constant flow rate of 20 ml min⁻¹, and the samples (20-25 mg) were heated from 25 to 600 °C at a rate of 10 °C min⁻¹.

The tensile properties of the samples were determined using a Hounsfield H5KS tensile tester at a crosshead speed of 100 mm min⁻¹ and 20 mm gauge length at ambient temperature. The samples were rectangular shaped with a width of 12 mm and thicknesses varying between 0.47 and 0.69 mm. At least five samples were tested for each composition and the mean values are reported. Young's modulus was predicted according to Nielsen's theoretical model [15-19].

The dynamic mechanical analysis (DMA) of the samples was done on a Perkin Elmer Diamond DMA dynamic mechanical analyzer. Rectangular shaped samples, with dimensions of 40 mm length, 10 mm width and thicknesses varying between 0.47 and 0.69 mm, were tested in tensile mode at a frequency of 1 Hz while heated under nitrogen flow from -100 to 100 °C at a rate of 3 °C min⁻¹.

3. Results and discussion

The SEM micrographs of cross-sections of the EPDM/SiO₂ composites are shown in Figures 1 to 3, while the particle size distributions are shown in Figure 4. The particle size distribution was determined from an average of 40 particles per sample. The light areas in the

micrographs correspond to the silica particles and are spherically shaped. The silica particles in the EPDM/SiO₂ samples are homogeneously dispersed in the rubber matrix and have good particle-matrix adhesion, which confirms the effectiveness of the *in situ* filler generation process used for the preparation of the filled rubbers.

The silica filled composites show both large and small particles at higher silica contents (Figure 3), and the particle size distribution determined from the visible particles confirms the increase in particle size (Figure 4). Figure 2 shows that some particles are fully imbedded in the EPDM matrix, which indicates good particle-matrix interaction. Increased agglomeration with increasing filler content has been observed and reported by other authors for similar systems [20-22], and is the result of increased coalescence of the growing silica particles when increasing the amount of *in situ* formed dispersed phase. The silica particles may also have agglomerated in the suspension, because the hydrophilic silica particles have a tendency to associate *via* hydrogen bonding [22]. When comparing these results with those obtained during our study on the same system, but with the samples prepared in the absence of a coupling agent [14], similar particle size distributions were observed. It is, however, difficult to draw any conclusions from this observation, since SEM analysis only shows the surface morphology of the investigated samples, and not enough particles could be measured to ensure statistically sound conclusions.

The FTIR spectra of EPDM, TESPT, EPDM-TESPT and the EPDM/SiO₂ composite containing 30 wt.% SiO₂ are shown in Figure 5. The neat rubber can be identified by two strong absorption peaks at 2920 cm⁻¹ and 2850 cm⁻¹ assigned to the C-H stretching vibration. The peaks at 721, 1376 and 1464 cm⁻¹ are assigned to the CH₂ stretching, and CH₃ and CH₂ bending, respectively [23,24]. The modification of the neat EPDM matrix with TESPT resulted in additional bands observed at 1073 and 952 cm⁻¹, both assigned to Si-O-CH₂CH₃ as a result of the asymmetric stretching of the Si-O group [25]. The FTIR spectrum for TESPT shows the following additional bands: asymmetric stretching of CH₃ (Si-O-CH₂CH₃) in the region 1390 cm⁻¹, CH₂CH₃ rocking of Si-O-CH₂CH₃ around 1167 cm⁻¹, band stretching of Si-C at 780 cm⁻¹, CH₂ wagging in CH₂-S- at 1246 cm⁻¹, and C-H stretching at 2373 cm⁻¹ [25].

TEOS undergoes hydrolysis by water to produce silanol groups (Si-OH) in the presence of the EPDM matrix during the sol-gel process. The silanol groups react with the ethoxysilane (Si-OCH₃CH₂) and produce siloxane groups. The ethoxy group (CH₃CH₂O) from TESPT can

also react with silanol to form a siloxane linkage. Networks of siloxane linkages will, therefore, form silica particles embedded in the rubber matrix. The siloxane linkage can be identified from the FTIR spectra of the vulcanized EPDM/SiO₂ composite as an asymmetric stretch (Si-O-Si) in the region 1055 cm⁻¹ (Figure 5). The vulcanized composite shows additional FTIR peaks at 803 and 944 cm⁻¹. They are assigned to Si-OH, which shows the presence of silanol groups, and to the asymmetric stretching of Si-O-C from unreacted TEOS [26-28]. The appearance of these functional groups implies that some of the silanol and ethoxysilane/ethoxy groups from both the TEOS and the coupling agent might have grafted on the rubber chains through reacting with the dicumyl peroxide initiator during vulcanization. The sulphide from the coupling agent has probably participated in sulphur vulcanization, as observed from the absence of a sulphide peak (CH₂-S-) for the EPDM/SiO₂ composite. The coupling agent probably formed bridges between the silica particles and the EPDM rubber, thereby leading to stronger chemical linkage between the silane coupling agent and the rubber molecule. The -OH bending vibration around 3300 cm⁻¹ is much weaker than that observed in the spectra of the samples prepared in the absence of coupling agent [14]. In the presence of coupling agent, the interaction between the EPDM rubber and the silica particles follows the reaction scheme proposed by Das *et al.* [1]. According to this scheme, the silanol groups are incorporated in the coupling agent generated crosslinks between the rubber chains. However, in the present case the silanol groups that formed part of the crosslinks obviously reacted further to form silica links, with the accompanying reduction in the number of free -OH groups.

The equilibrium swelling and gel content results of the vulcanized EPDM and the EPDM/SiO₂ composites are reported in Table 1. Equilibrium swelling analysis is well-known to evaluate the crosslink density obtained after vulcanization of an unfilled rubber. In the case of silica filled rubber composites, the swelling behaviour could be influenced by (1) the ability of the silica particles to act as crosslinking points and/or absorb solvent, and (2) the degree of crosslinking of the unfilled rubber matrix.

Table 1 Swelling ratio and gel content of EPDM and EPDM/SiO₂ composites

Samples (w/w)	q	q_{EPDM}	$f / \%$	$f_{EPDM} / \%$	Gel / %
EPDM	3.7 ± 0.2	3.7 ± 0.2	6.4 ± 2.5	6.4 ± 2.5	93.6 ± 2.5
90/10 EPDM/SiO ₂	5.9 ± 0.6	6.6 ± 0.6	1.8 ± 0.4	2.0 ± 0.4	98.2 ± 0.3

80/20 EPDM/SiO ₂	4.3 ± 0.6	5.0 ± 0.7	3.0 ± 1.6	3.6 ± 1.9	96.2 ± 2.0
70/30 EPDM/SiO ₂	4.3 ± 0.0	6.0 ± 0.0	2.5 ± 1.5	3.6 ± 2.2	96.4 ± 2.2

Swelling ratios (q and q_{EPDM}), extractable fraction (f and f_{EPDM}) and gel content for EPDM and EPDM/SiO₂ nanocomposites

The normalised swelling ratio in Table 1 shows an increase for the silica containing samples, while the gel content remained effectively constant. This indicates that the number of crosslinks decreased, while the network is still extensive enough to maintain the high gel content. Another possibility is that longer chain crosslinks have been formed between the rubber chains (as proposed by Das *et al.* [1]). In this case, an extensive network will still exist but there will be enough free volume between the chains to accommodate the toluene molecules during the swelling test, which explains the increase in swelling ratios. In our previous paper [14] where the nanocomposites were prepared in the absence of a coupling agent we also observed an increase in swelling ratio, but in that case the extractable fraction increased and the gel content decreased significantly, which clearly showed inhibition of the rubber crosslinking in the presence of silica nanoparticles. In this case, the silica particles became part of the crosslinks through the action of the coupling agent [1]. The introduction of TESPT has, therefore, an influence on the effectiveness of crosslinking and on the length of the crosslinks in the vulcanized EPDM/SiO₂ composites

The TGA curves of EPDM rubber and silica filled composites are shown in Figure 6. The thermal stability was characterized through temperatures taken at the onset and at 50% mass loss (Table 2). The TGA curves of the EPDM/SiO₂ nanocomposites clearly show two distinct mass loss steps, and an increasing amount of char with increasing silica content (Figure 6 and Table 2). The first mass loss is observed from 100 °C and is due to a loss of water and alcohol, and progresses to higher temperatures due to the presence of organic by-products such as unhydrolyzed TEOS that decompose and evaporate around 350 °C. The second mass loss around 400-470 °C is related to the main degradation of EPDM rubber chains or segments. The degradation temperatures of EPDM initially decrease for the 10% silica containing sample, but increase to temperatures higher than that of EPDM for the samples containing 20 and 30% silica (Table 2). The introduction of the coupling agent obviously improved the interaction with and dispersion of silica particles in the EPDM matrix, which gave rise to the increased thermal stability of the EPDM. The strongly bound and well dispersed silica particles reduced polymer chain mobility and retarded the diffusion of volatile products from the sample. It probably also changed the decomposition mechanism

of EPDM, similar to that reported in other thermal degradation studies [7,29-32]. Our previous results, obtained in the absence of a coupling agent, showed very little influence of the silica filler on the thermal stability of the matrix.

The actual silica content after conversion was determined through TGA analysis as the percentage residue after heating to 600 °C. The data in Table 2 show a very good correlation between the % residue and the amount of silica introduced through the sol-gel reaction. The small standard deviation values in Table 2 indicate that the silica particles were well dispersed in the rubber matrix, because samples were taken from different positions in the pressed sheets for the repeat TGA analyses.

Table 2 Summary of TGA results for the EPDM rubber and its composites

Samples (w/w)	T _{onset} / °C	T _{50 %} / °C	% SiO ₂
EPDM	426 ± 0.1	454 ± 0.1	0
90/10 EPDM/SiO ₂	420 ± 2.7	452 ± 1.3	9.0 ± 0.4
80/20 EPDM/SiO ₂	435 ± 1.6	463 ± 3.4	19.1 ± 2.3
70/30 EPDM/SiO ₂	436 ± 2.8	469 ± 0.1	29.0 ± 0.7

T_{onset} and T_{50%} are the temperatures at the onset and at 50% mass loss

The Young's modulus as function of volume fraction of neat EPDM and its silica filled composites are shown in Figure 7, together with its prediction according to the Nielsen theoretical model [15-19]. The values for Young's modulus, stress and elongation at break, are summarized in Table 3. For composite materials consisting of spherical particles in the matrix, the Nielsen equation has the form given in Equations 8 and 9.

$$E = E_1 \left[\frac{1 + AB\phi_2}{1 - B\phi_2} \right] \quad (8)$$

$$B = \frac{\frac{E_2}{E_1} - 1}{\frac{E_2}{E_1} + A} \quad (9)$$

where E , E_2 and E_1 are the modulus values of the composite, filler and matrix respectively, and ϕ_2 is the volume fraction of the filler assuming spherical particles. The theoretical

modulus used for the silica particles was $E_2 = 70$ GPa [33]. The factor ψ takes into account the values of ϕ_m of the dispersed phase, and it is given by Equation 10.

$$\psi = 1 + \left[\left(\frac{1 - \phi_m}{\phi_m} \right) \phi_a \right] \quad (10)$$

where ϕ_m is the maximum packing fraction. The constant B takes into account the relative moduli of the filler and matrix phases, and its value is 1.0 for very large E_2/E_1 ratios (the values for E_2 and E_1 are 70 GPa and 2.4 MPa, respectively, and therefore we could confidently use a value of 1.0). The constant A is related to the Einstein coefficient given by Equation 11 and is determined by the morphology of the system; for strong aggregates, the value of A can become quite large while ϕ_m of the dispersed phase will decrease.

$$A = k_E - 1 \quad (11)$$

An A value of 4.5 gave the best fit of the experimental modulus values (Figure 7). It is interesting to observe that the addition of TESPT reduced the values of A and ϕ_m significantly when compared to our previous study, where the same system in the absence of a coupling agent was investigated [14]. The values of A and ϕ_m were then 25 and 0.37, respectively,

which indicated a large extent of silica aggregation in the EPDM matrix with increasing silica content. Furthermore, the silica aggregates were large enough to increase the value of A and

reduce the value of ϕ_m . In the current study, the introduction of a coupling agent improved the

dispersion of the filler and reduced the size of the aggregates, as was also observed from the

SEM images in Figures 1 to 3. The low value of ϕ_m indicates the presence of agglomerated

silica particles, but the aggregates are small enough for the value of A to be significantly reduced.

Table 3 Summary of tensile results of EPDM and the EPDM/SiO₂ composites

Samples	σ_b / MPa	ε_b / %	E / MPa
EPDM	1.7 ± 0.5	482 ± 84	2.4 ± 0.3
90/10 w/w EPDM/SiO ₂	3.1 ± 0.4	763 ± 62.9	5.0 ± 0.6
80/20 w/w EPDM/SiO ₂	3.7 ± 0.7	1060 ± 20.0	7.4 ± 0.3
70/30 w/w EPDM/SiO ₂	3.2 ± 0.4	730 ± 28.9	18.7 ± 1.0

ε_b , σ_b , and E are elongation at break, stress at break, and Young's modulus of elasticity

It is also interesting to observe that both the stress and elongation at break increase with increasing filler content for 10 and 20 wt.% silica (Table 3). This is the result of improved adhesion between the filler and the matrix because of good interfacial interaction brought about by the coupling agent, giving rise to effective stress transfer. Das *et al.* [1] also reported high stress and elongation at break values in their investigation of silica-EPDM rubber networks by an *in situ* sol-gel method. They explained this as the polysulfidic linkage from the TESPT causing a strong reinforcement between the rubber and the filler, which explains the larger stress at break values. The longer crosslink chains formed in the presence of the coupling agent explain the larger elongation at break values. A larger amount of filler led to agglomeration of the filler particles, which resulted in a decrease in the stress and elongation at break for the sample containing 30 wt.% silica. In this case, there were probably silica

particles that were not incorporated in the crosslinks through the action of the coupling agent, and that formed agglomerates acting as stress concentration points. Aggregation of the filler in the composite probably caused a dewetting or crazing effect in which the adhesion between the filler and matrix phase was destroyed, and this resulted in a decline in the mechanical properties. When comparing these results with those obtained during our study on the same system, but with the samples prepared in the absence of a coupling agent [14], it is observed that the tensile modulus values for the different nanocomposites, prepared in the absence and presence of TESPT, are similar, but that the stress and elongation at break values for the samples prepared in the presence of TESPT are significantly higher. This can also be explained by the better interaction between the rubber chains and the silica particles incorporated in the crosslinks [1], which improved the interfacial interaction and reduced the number of stress concentration points, and by the longer crosslink chains, which increased the strain-ability of the nanocomposites.

The DMA results of EPDM and its nanocomposites are shown in Figure 8. The glass transition temperature, the $\tan \delta$ value at the glass transition peak maximum, the storage modulus at 50 °C, Factor C and the damping reduction values are summarized in Table 4. From the values of the storage modulus obtained in the glassy and rubbery regions, the filler effectiveness (Factor C) in the rubber matrix can be evaluated from Equation 12 [35].

$$\text{Factor } C = \frac{\left(\frac{E'_g}{E'_r} \right)_{\text{composites}}}{\left(\frac{E'_g}{E'_r} \right)_{\text{matrix}}} \quad (12)$$

where, E'_g and E'_r are the storage moduli determined in the glassy and rubbery regions, respectively. The state of filler dispersion in the rubber matrix was determined by calculation of the damping reduction (DR) from the normalised damping values obtained from the maxima of the $\tan \delta$ peaks ($\tan \delta_{\text{rubber}}$ and $\tan \delta_{\text{composite}}$), and is given by Equation 13 [35].

$$DR = \frac{\tan \delta_{EPDM} - \tan \delta_{\text{composite}}}{\tan \delta_{EPDM}} \times 100\% \quad (13)$$

In the rubbery region, there is a significant increase in the storage modulus with increasing silica content in the vulcanizates (see $E'_{T=50^\circ\text{C}}$ values in Table 4). These modulus values depend on both the degree of crosslinking of the rubber matrix and the content of the

rigid dispersed phase. Both these factors will contribute to an increase in modulus. As can be seen from Table 1, the degree of crosslinking remained fairly constant with increasing silica content (see q_{EPDM} values for filled samples). However, the content of the rigid dispersed phase increased significantly and the interaction between the rubber and filler was very good because of the presence of coupling agent during the preparation of the composites. These factors gave rise to much higher storage modulus values that correlate well with the tensile modulus values in Table 3. The modulus values, reported in Table 4, are very similar to those reported for the same samples prepared in the absence of a coupling agent [14]. This indicates that the rigidity of the fillers makes the biggest contribution to the elastic modulus of the EPDM nanocomposites.

Table 4 Summary of DMA results of EPDM and EPDM/SiO₂ composites

Samples (w/w)	$E'_{T=50^{\circ}\text{C}}$ / MPa	$\tan \delta_{\max}^{\text{Norm}}$	T_g / °C	Factor C	DR / %
EPDM	3.2	0.622	-41.5	1	-
90/10 EPDM	6.0	0.603	-41.9	0.77	3.1
80/20 EPDM	12.0	0.390	-42.5	0.18	37.3
70/30 EPDM	24.5	0.363	-42.3	0.11	41.6

$E'_{T=50^{\circ}\text{C}}$, $\tan \delta_{\max}^{\text{Norm}}$, T_g , Factor C and DR^{Norm} are the modulus at 50 °C, maximum $\tan \delta$ (normalised to the amount of rubber in the nanocomposites), glass transition temperature, filler effectiveness and the damping reduction (calculated from $\tan \delta_{\max}^{\text{Norm}}$)

The filler effectiveness (Factor C) (Table 4) can be used to indicate the composite reinforcing capacity. By definition, an unfilled rubber matrix has a Factor C equal to 1, and a Factor C lower than 1 indicates a mechanical stiffening effect as well as a thermal stability contribution of the filler [35]. The values in Table 4 clearly show that the silica particles contributed to the EPDM matrix stiffness as the silica content increases.

The addition of rigid fillers to a polymer matrix is expected to restrict the mobility of the polymer chains, leading to a decrease in damping and a shift in the glass transition temperature to higher values. The normalized $\tan \delta$ values in Table 4 clearly decrease with increasing silica content. The decrease in the damping factor is attributed to good adhesion between the filler and the matrix, which resulted in restriction in the mobility of rubber chains

in the composite. The increasing damping reduction (DR^{Norm}) values with increasing silica content confirm that the EPDM interacts strongly with the well dispersed silica particles, which leads to a reduction in polymer chain mobility. The glass transition temperature slightly increased for the silica containing samples, which is expected because of the reduced chain mobility of EPDM in the nanocomposites.

3. Conclusions

Reinforcing of EPDM rubber with *in situ* generated silica particles in the presence of a coupling agent (TESPT) *via* a sol-gel route was investigated. The silica filled composites showed both large and small particles at higher silica contents in the composites, and some particles were fully imbedded in the EPDM matrix, which indicated good particle-matrix interactions. The particle size distribution increased with increasing silica content as a result of increased coalescence of the growing silica particles when increasing the amount of *in situ* formed dispersed phase. The FTIR results indicate that the TEOS and TESPT reacted to form silica containing crosslinks between the rubber chains. In the presence of the silica particles, there was a decrease in crosslink density, but the networks were still extensive enough to maintain a high gel content. The introduction of the coupling agent improved the interaction of the silica particles with, and dispersion in, the EPDM matrix, which gave rise to an increased thermal stability of the EPDM. The tensile results showed that longer crosslink chains formed in the presence of the coupling agent gave rise to larger elongation at break values, and the polysulfidic linkage from the TESPT produced strong reinforcement between the rubber and the filler, which gave rise to the larger stress at break values. However, larger amounts of filler led to agglomeration of the filler particles, which resulted in a decrease in the stress and elongation at break. A Nielsen's model fit to the Young's modulus values shows improved dispersion and reduced size of the silica aggregates in the EPDM matrix. There is good correlation between the storage modulus and Young's modulus, and these values increased significantly with increasing filler content. The increased stiffness and thermal stability are confirmed by the filler effectiveness factor values. The damping reduction values confirm that the EPDM interacted strongly with the well dispersed silica particles, which led to a reduction in the polymer chain mobility. When the results of this study are compared with those of our previous study on the same system in the absence of a coupling agent, it is clear that the introduction of the coupling agent improved the interaction and dispersion of silica particles in the EPDM matrix, and had an influence on the

effectiveness of crosslinking and on the length of the crosslinks in the vulcanized EPDM/SiO₂ composites. Because of this influence, the EPDM/silica nanocomposites showed much better thermal and mechanical properties.

Acknowledgements

The National Research Foundation in South Africa and the University of the Free State are acknowledged for financial support of the project. The Italian Ministry of Foreign Affairs (Italy-South Africa bilateral collaboration project) for financial support of the project.

4. References

1. A. Das, R. Jurk, K.W. Stöckelhuber, G. Heinrich. Silica-ethylene propylene diene monomer rubber networking by in situ sol-gel method. *Journal of Macromolecular Science, Part A: Pure and Applied Chemistry* 2008; 45:101-106.
DOI: 10.1080/10601320701683447
2. Y. Ikeda, A. Tanakaa, S. Kohjiya. Effect of catalyst on in situ silica reinforcement of styrene-butadiene rubber vulcanizate by the sol-gel reaction of tetraethoxysilane. *Journal of Materials Chemistry* 1997; 7:455-458.
3. K. Murakami, S. Iio, Y. Ikeda, H. Ito, M. Tosaka, S. Kohjiya. Effect of silane-coupling agent on natural rubber filled with silica generated in situ. *Journal of Materials Science* 2003; 38:1447-1455.
4. S. Kohjiya, Y. Ikeda. In situ formation of particulate silica in natural rubber matrix by the sol-gel reaction. *Journal of Sol-Gel Science and Technology* 2003; 26:495-498.
DOI: 10.1023/A:1020743214628
5. Y. Ikeda, S. Kohjiya. In situ formed silica particles in rubber vulcanizate by the sol-gel method. *Polymer* 1997; 38:4417-4423.
6. M. Messori. In situ synthesis of rubber nanocomposites. *Advanced Structured Materials* 2011; 9:57-85.
DOI: 10.1007/978-3-642-15787-5_2

7. T.E. Motaung, A.S. Luyt, S. Thomas. Morphology and properties of NR/EPDM rubber blends filled with small amounts of titania nanoparticles. *Polymer Composites* 2011; 32:1289-1296.
DOI: 10.1002/pc.21150
8. D. Fragiadakis, L. Bokobza, P. Pissis. Dynamics near the filler surface in natural rubber-silica nanocomposites. *Polymer* 2011; 52:3175-3182.
DOI:10.1016/j.polymer.2011.04.045
9. R. Scotti, L. Wahba, M. Crippa, M. D'Arienzo, R. Donetti, N. Santod, F. Morazzoni. Rubber-silica nanocomposites obtained by in situ sol-gel method: Particle shape influence on the filler-filler and filler-rubber interactions. *Soft Matter* 2012; 8:2131-2143.
DOI: 10.1039/c1sm06716h
10. L. Bokobza. The reinforcement of elastomeric networks by fillers. *Macromolecular Materials and Engineering* 2004; 289:607-621.
DOI: 10.1002/mame.200400034
11. V. Tangpasuthadol, A. Intasiri, D. Nuntivanich, N. Niyompanich, S. Kiatkamjornwong. Silica-reinforced natural rubber prepared by the sol-gel process of ethoxysilanes in rubber latex. *Journal of Applied Polymer Science* 2008; 109:424-433.
DOI: 10.1002/app.28120
12. L. Bokobza, J.-P. Chauvin. Reinforcement of natural rubber: Use of *in situ* generated silicas and nanofibres of sepiolite. *Polymer* 2005; 46:4144-4151.
DOI: 10.1016/j.polymer.2005.02.048
13. D. Morselli, F. Bondioli, A.S. Luyt, T.H. Mokhothu, M. Messori. Preparation and characterization of EPDM rubber modified with *in situ* generated silica. *Journal of Applied Polymer Science* 2012; 128: 2525-2532.
DOI: 10.1002/app.38566
14. T.H. Mokhothu, A.S. Luyt, D. Morselli, F. Bondioli, M. Messori. Influence of *in situ* generated silica nanoparticles on EPDM morphology, thermal, thermomechanical and mechanical properties. Submitted for publication in *Polymer Composites*.
15. L.E. Nielsen. Morphology and elastic modulus of block polymers and polyblends. *Rheological Acta* 1974; 13:86-92.
16. L.E Nielsen, R.F. Landel. *Mechanical Properties of Polymers and Composites*. Marcel Dekker, Inc.: New York (1994).
ISBN: 0 8247 8964 4

17. Y.-P. Wu, Q.-X. Jia, D.-S. Yu, L.-Q. Zhang. Modeling Young's modulus of rubber-clay nanocomposites using composite theories. *Polymer Testing* 2004; 23:903-909.
DOI: 10.1016/j.polymertesting.2004.05.004
18. T.K. Jayasree, P. Predeep. Effect of filler on mechanical properties of dynamically crosslinked styrene butadiene rubber/high density polyethylene blends. *Journal of Elastomers and Plastics* 2008; 40:127-146.
DOI: 10.1177/0095244307083865
19. S. Ahmed, F.R. Jones. A review of particulate reinforcement theories for polymer composites. *Journal of Materials Science* 1990; 25:4933-4942.
20. M. Messori, F. Bignotti, R. De Santis, R. Taurino. Modification of isoprene rubber by *in situ* silica generation. *Polymer International* 2009; 58:880-887.
DOI: 10.1002/pi.2606
21. Y. Ikeda, Y. Kameda. Preparation of "green" composites by the sol-gel process: *In situ* filled natural rubber. *Journal of Sol-Gel Science and Technology* 2004; 31:137-142.
DOI: 10.1023/B:JSST.0000047975.48812.1b
22. S. Prasertsri, N. Tattanasom. Mechanical and damping properties of silica/natural rubber composites prepared from latex system. *Polymer Testing* 2011; 30:515-526.
DOI: 10.1016/j.polymertesting.2011.04.001
23. G.M.O. Barra, J.S. Crespo, J.R. Bertolino, V. Soldi, A.T.N. Pires. Maleic anhydride grafting on EPDM: Qualitative and quantitative determination. *Journal of Brazilian Chemical Society*, 1999; 10:31-34.
24. A.I. Hussain, M.L. Tawfic, A.A. Khalil, T.E. Awad. High performance emulsified EPDM grafted with vinyl acetate as compatibilizer for EPDM with polar rubber. *Nature and Science* 2010; 8:348-357.
25. D. Zhu, W.J. van Ooij. Structural characterization of bis-[triethoxysilylpropyl] tetrasulfide and bis-[trimethoxysilylpropyl]amine silanes by Fourier-transform infrared spectroscopy and electrochemical impedance spectroscopy. *Journal of Adhesion Science and Technology* 2002; 16:1235-1260.
DOI: 10.1163/156856102320256873
26. A. Bandyopadhyay, A.K. Bhowmick, M. De Sarkar. Synthesis and characterization of acrylic rubber/silica hybrid composites prepared by sol-gel technique. *Journal of Applied Polymer Science* 2004; 93:2579-2589.
DOI: 10.1002/app.20681

27. M.A. De Luca, M.M. Jacobi, L.F. Orlandini. Synthesis and characterisation of elastomeric composites prepared from epoxidised styrene butadiene rubber, 3-aminopropyltriethoxysilane and tetraethoxysilane. *Journal of Sol-Gel Science and Technology* 2009; 49:150-158.
DOI: 10.1007/s10971-008-1851-8
28. N.D. Meeks, S. Rankin, D. Bhattacharyya. Sulfur-functionalization of porous silica particles and application to mercury vapor sorption. *Industrial and Engineering Chemistry Research* 2010; 49:4687-4693.
DOI: 10.1021/ie901580k
29. Q. Ji, X. Wang, Y. Zhang, Q. Kong, Y. Xia. Characterization of poly(ethylene terephthalate)/SiO₂ nanocomposites prepared by sol-gel method. *Composites: Part A* 2009; 40:878-882.
DOI: 10.1016/j.compositesa.2009.04.010
30. K. Chrissafis, D. Bikiaris. Can nanoparticles really enhance thermal stability of polymers? Part I: An overview on the thermal decomposition of addition polymers. *Thermochimica Acta* 2011; 523:1-24.
DOI: 10.1016/j.tca.2011.06.010
31. D. Bikiaris. Can nanoparticles really enhance thermal stability of polymers? Part II: An overview on the thermal decomposition of polycondensation polymers. *Thermochimica Acta* 2011; 523:25-45.
DOI: 10.1016/j.tca.2011.06.012
32. T.K. Dey, M. Tripathi. Thermal properties of silicon powder filled high-density polyethylene composites. *Thermochimica Acta* 2010; 502:35-42.
DOI: 10.1016/j.tca.2010.02.002.
33. T.H. Hsieh, A.J. Kinloch, K. Masania, J.S. Lee, A.C. Taylor, S. Sprenger. The toughness of epoxy polymers and fibre composites modified with rubber microparticles and silica nanoparticles. *Journal of Materials Science* 2010; 45:1193-1210.
DOI: 10.1007/s10853-009-4064-9
34. R. Tlili, V. Cecen, I. Krupa, A. Boudenne, L. Ibos, Y. Candau, I. Novák. Mechanical and thermophysical properties of EVA copolymer filled with nickel particles. *Polymer Composites* 2011; 32:727-736.
DOI: 10.1002/pc.21091
35. A. Gregorova, M. Machovsky, R. Wimmer. Viscoelastic properties of mineral-filled poly(lactic acid) composites. *International Journal of Polymer Science* 2012; 2012:1-6.

DOI: 10.1155/2012/252981

ACCEPTED MANUSCRIPT

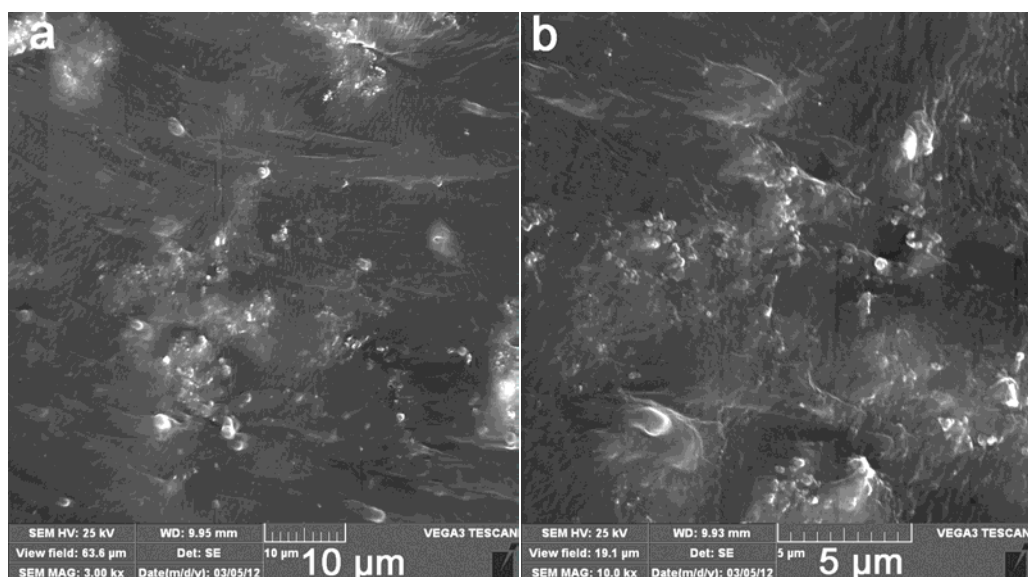


Figure 1 SEM micrographs of the 90/10 w/w EPDM/SiO₂ composite

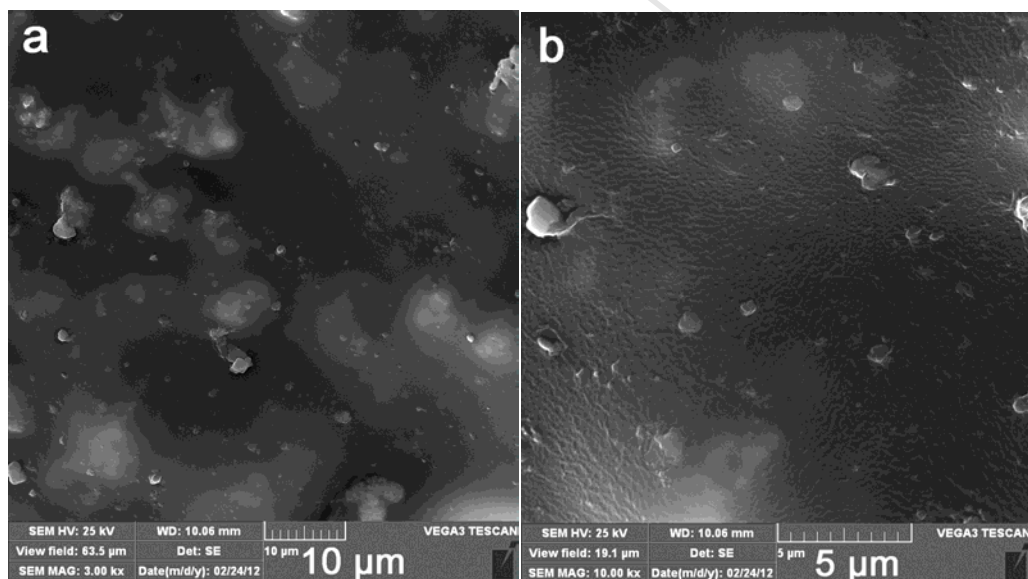


Figure 2 SEM micrographs of the 80/20 w/w EPDM/SiO₂ composite

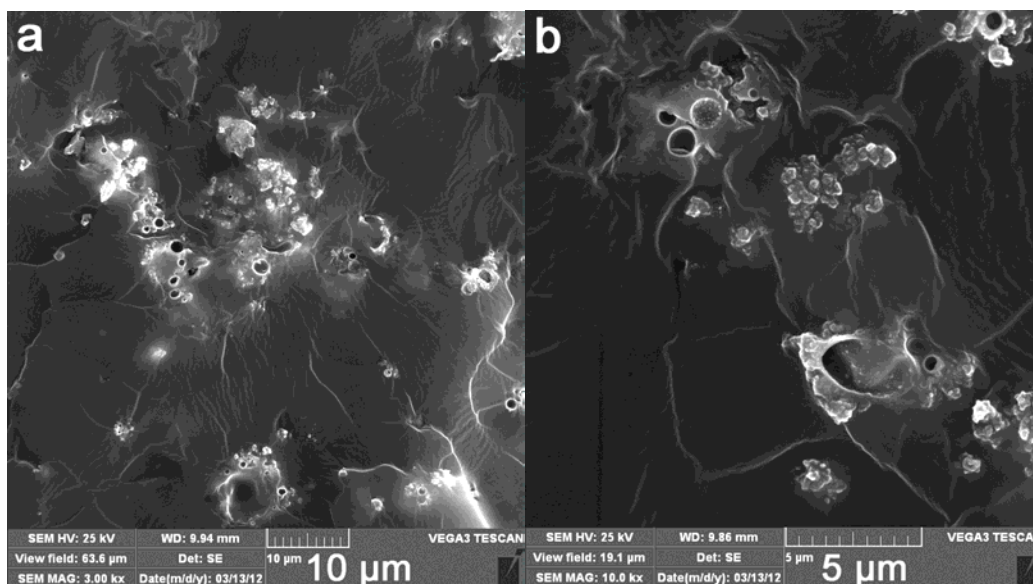


Figure 3 SEM micrographs of the 70/30 w/w EPDM/SiO₂ composite

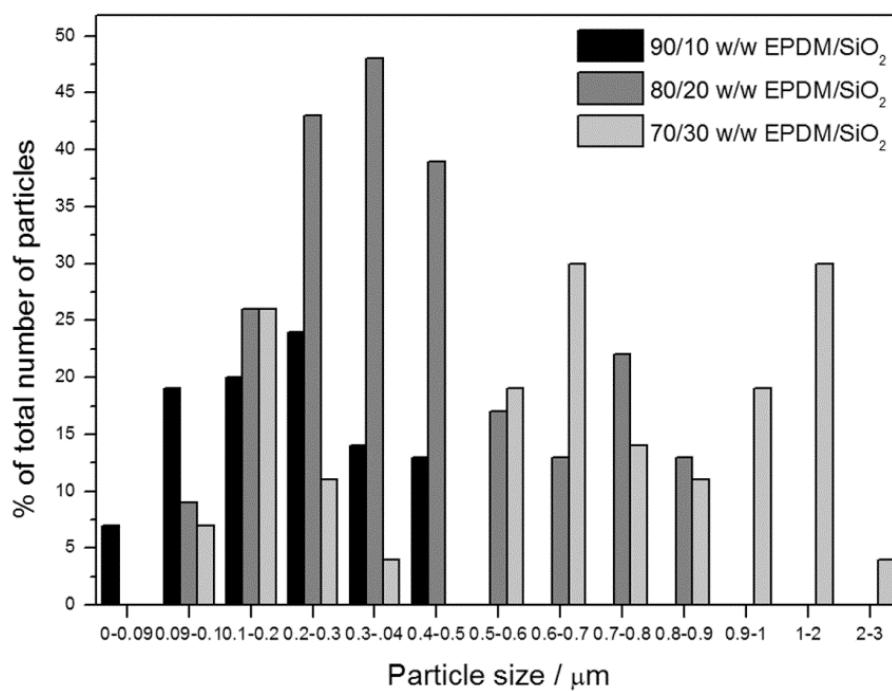


Figure 4 Particle size distribution graphs of the EPDM/SiO₂ composites

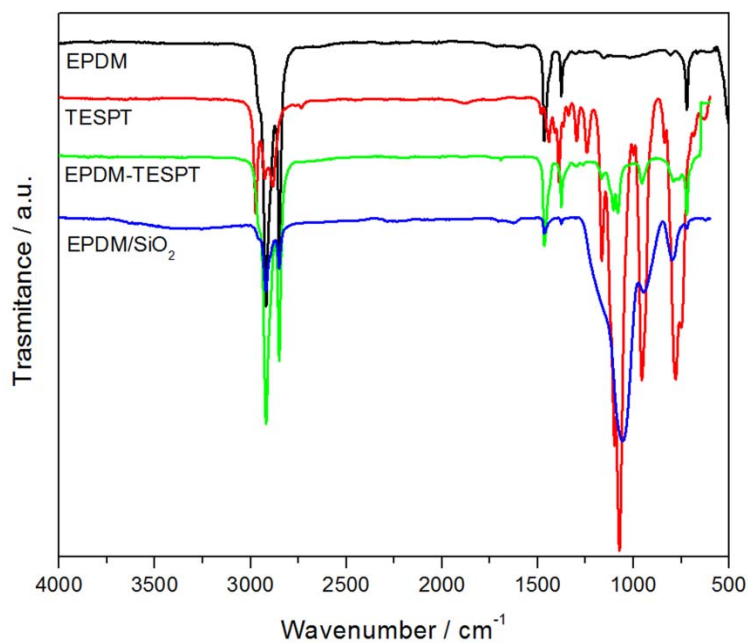


Figure 5 FTIR spectra of EPDM, TESPT, EPDM-TESPT and the EPDM/SiO₂ composite containing 30 wt.% silica

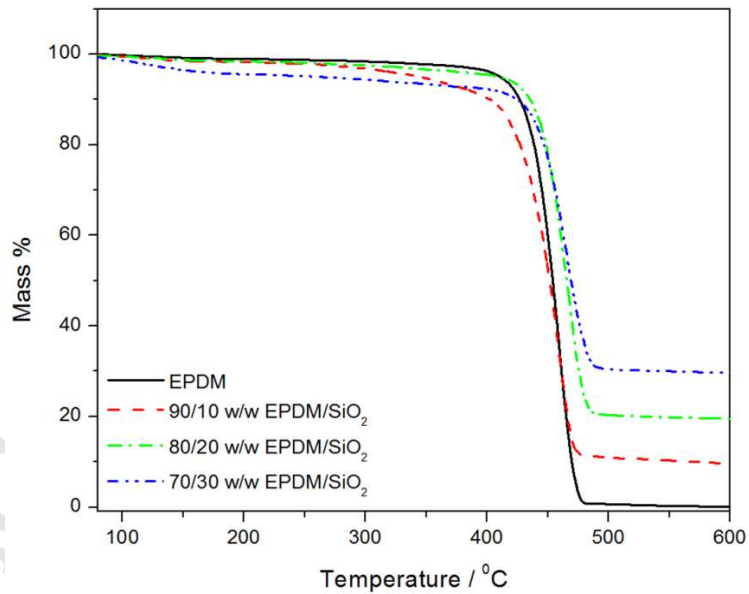


Figure 6 TGA curves of EPDM and silica filled EPDM composites

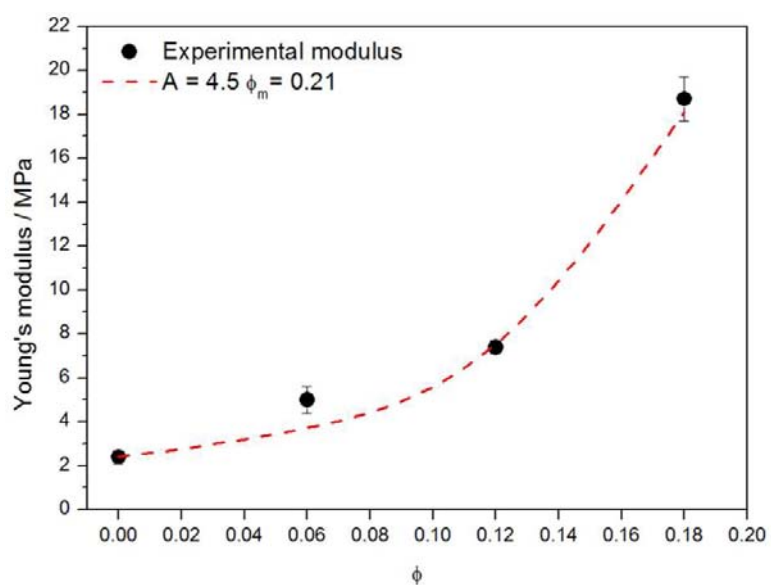


Figure 7 Young's modulus as a function of volume fraction of SiO₂ in EPDM/SiO₂ composites: experimental modulus and Nielsen predicted modulus

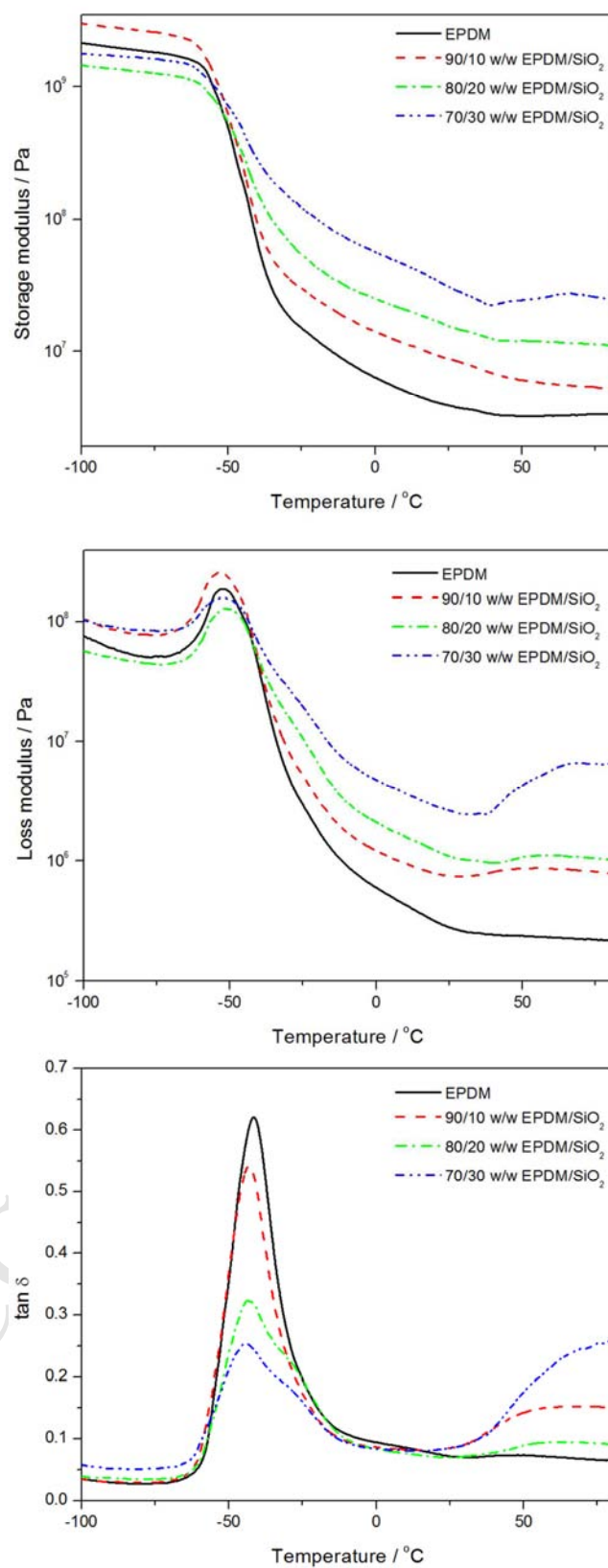


Figure 8 DMA storage modulus, loss modulus and damping factor curves of EPDM and its composites